Removal of Cu^{2+} in solution by using composite of pyrite-alginate

Muhammad Wahyu Nugraha[1], Muhammad Aziz bin Shamsul Ariffin[2], Suriati Sufian[2], Dita Floresyona[3], Nonni Soraya Sambudi[3]

{mwahyungrh@s.okayama-u.ac.jp[1], muhammad_17004746@utp.edu.my[2], suriati@utp.edu.my[2], dita.floresyona@universitaspertamina.ac.id[3], nonni.ss@universitaspertamina.ac.id[3]}

Department of Chemistry, Graduate School of Natural Science and Technology, Okayama University, Okayama 700-8530, Japan[1], Department of Chemical Engineering, Universiti Teknologi PETRONAS, Seri Iskandar, 32610 Perak, Malaysia[2], Department of Chemical Engineering, Universitas Pertamina, Simprug, Jakarta Selatan 12220, Indonesia[3]

Abstract. Heavy metals with high level of toxicity have negative impact on public health and the environment. In this research, Cu^{2+} as a type of heavy metal was removed by using synthesized oxalate pyrite-alginate beads as an adsorbent. Pyrite is abundant in nature, and considered to be an omnipresent mineral. It is then functionalized with oxalate to improve its colloidal stability and increase its surface charge. The impacts of bead amount on Cu^{2+} adsorption, initial Cu^{2+} concentration, and recyclability test are three parameters that were studied in batch adsorption experiments. The highest removal of Cu^{2+} can be achieved at 96.66% for 5 ppm Cu^{2+} solution using 3 g of oxalate pyrite-alginate beads. The beads still can maintain the adsorption efficiency of 66.4% after 5 cycles of usage. The adsorption is best fitted in Freundlich isotherm. Hence, the composite shows high potential for heavy metals removal, especially Cu^{2+} from aqueous environment.

Keywords: Cu^{2+}, Adsorption, Pyrite, Oxalate, Alginate.

1 Introduction

Heavy metals, particularly copper, mercury, chromium, and cadmium, are considered as one of the most significant environmental issues, as they are commonly found in high concentrations in contaminated streams and soils. Heavy metal concentrations contained in the effluents pollute river water and contaminate fish, which eventually creates significant health risks [1], [2]. Copper is used in various industrial and agricultural operations and released into the environment through a variety of sources, including mining, metal piping, chemical manufacturing, and pesticide manufacturing [3]. Copper is one of the trace metals that, in low concentrations, is vitally important for humans, plants, and animals. Though our body needs some heavy metals such as copper and zinc; in high concentration due to human industrialization, the presence of these metals may cause hazardous effects such as increased blood pressure and respiratory rates, damage in kidney and liver, which abrupt the metabolic

ICO-SEID 2022, November 23-24, Jakarta, Indonesia

DOI 10.4108/eai.23-11-2022.2339151

process and can even lead to death [3], [4]. Hence, copper ions need to be removed before being discharged to the environment to prevent negative repercussions.

Since heavy metals tend to accumulate along the food chain and are uncontrollable for biological degradation, treatment processes are continually implemented and developed to remove them from the wastewater such as reverse osmosis [5], ion exchange [6], chemical precipitation [7], and solvent extraction [8]. Adsorption is known as one of the most effective, economical, and simple methods for heavy metal removal from aqueous solutions [9]. Besides, the benefits of this method include the ability of adsorbents to regenerate and to be reused, as well as the recovery of adsorbate metal ions.

Pyrite (FeS_2) with a huge geological reserve is a kind of iron sulfide that is widely dispersed in the Earth's surface region and due to the high affinity of the sulfur element, pyrite has emerged as a type of low-cost sorbent material [10]. Natural pyrite has been regarded as a kind of potential sorbent to control mercury emission from coal-fired power plants because of its low cost and high affinity [11]. Pyrite has also been used to reduce high mobility hexavalent chromium (Cr(VI)) to relatively non-toxic trivalent chromium (Cr(III)) [12], [13], which pyrite showed strong reducing capacity and high adsorption capacity [14]. Previous study by Ozverdi and Erdem [15] has shown the ability of pyrite to adsorb Cu^{2+}, Cd^{2+}, and Pb^{2+} from aqueous solution, in which, the interaction of metal and surface Fe and S atoms determined the adsorption effectiveness [16]. To improve the sustainability of pyrite used for heavy metals adsorption, immobilization of pyrite through composite synthesis can serve as a solution, especially in improving the recyclability of material.

Alginate as a natural polysaccharide contains abundant amounts of hydroxyl and carboxyl groups, which facilitate the physical and chemical interactions with heavy metals [17], [18]. Various studies on adsorptions of copper (II) by using alginate show high removal rate with oxygen atoms of alginate easily form covalent bonds with the metal ions with strong electronegativity [19]. Hence, combination of pyrite and alginate produces adsorbent with excellent sorption ability. In order to achieve high distribution of pyrite in alginate, pyrite is functionalized with oxalate. During the functionalization of iron nanoparticles, the exposed carboxylic acid group will provide the nanoparticles with hydrophilic properties, reduce clustering of nanoparticles and act as an unrestrained point to further surface modification [20]. The combination of oxalate modified pyrite with alginate has not been researched before hand for the adsorption of heavy metal. In this study, we will observe the effect of adsorbent amount, adsorbate concentration, and recyclability of composite material for adsorption process.

2 Methodology

2.1 Materials

Oxalic acid dihydrate ($C_2H_6O_6$), sodium alginate, and calcium chloride ($CaCl_2$) were purchased from R&M Chemical (India). Ferrous sulfate ($FeSO_4$), Sigma Aldrich (USA), ethanol (C_2H_5OH), HmBG (Malaysia), copper (II) sulfate-5-hydrate ($CuSO_4.5H_2O$), and Bendosen (Malaysia) were purchased from various vendors. Copper solution was prepared by dissolving $CuSO_4.5H_2O$ in de-ionized (DI) water. All chemicals were analytical reagent grade and used

without any further purification. PureLab Flex® (ELGA, France) DI water (18.2 M) was used throughout the experiment.

2.2 Methods

2.2.1 Oxalate pyrite synthesis

The pyrite was synthesized using hydrothermal method from the previous study reported by Sun with some modifications [21]. Typically, 100 mL of 0.0566 mol oxalic acid dihydrate was dispersed into 100 mL of 0.1017 ferrous sulfates until mixed thoroughly. Subsequently, 8 mL ethanol was added to the mixture to reduce the particle size. Afterwards, the mixture was undergone hydrothermal treatment at 120 ℃ for 30 min. The solution was cooled down and filtered using vacuum filtration. Afterwards, the pyrite was washed several times using DI water and dried at 80 ℃ overnight.

2.2.2 Oxalate pyrite – alginate beads composite synthesis

The beads composite was prepared using the co-precipitation method from previous work [18], [22]. In a typical preparation, 5 g sodium alginate powder was dissolved into 100 mL DI water. 1 g of oxalate pyrite was added to the solution and stirred for 3 h. Consecutively, the mixture was added dropwise using a syringe into 500 mL of 10 g/L calcium chloride. Afterwards, the as-prepared bead composite was washed several times with DI water to remove excess calcium chloride and dried at room temperature for several hours.

2.2.3 Batch adsorption studies

Typically 0.5 g of oxalate pyrite-alginate beads were mixed with 5 ppm of 100 mL copper solution. The solution was shaken using a mechanical shaker at 175 rpm for 8 h, while a 15 mL sample was taken at a certain interval time to be analyzed using Agilent 240 FS AAS (Atomic Absorption Spectroscopy). The effect of oxalate pyrite-alginate beads concentrations was analyzed using different concentrations, i.e., 1 g, 2 g, and 3 g. Furthermore, the effect of initial copper concentrations was also investigated using the best beads composite concentration. The different copper concentrations that were used are 10, 15, and 20 ppm.

The recyclability of the composite was analyzed using a 5 ppm copper solution. After each cycle, the beads composite was washed thoroughly with DI water before starting the next cycle.

2.2.4 Characterizations

The surface and particle morphology and chemical composition was analyzed using Zeiss EVOLS15 SEM/ EDX (Scanning electron microscopy/ Energy-dispersive X-ray). The functional group was characterized using Perkin Elmer Spectrum One FTIR–ATR (Fourier Transform Infrared Spectroscopy– Attenuated Total Reflectance). The spectra are recorded in the reflection of 4000-500 cm^{-1} range from 8 scans with a resolution of 4 cm^{-1}. The crystallinity phase of the composite was investigated using Bruker D8 on X′Pert3 Powder and Empyrean PANalytical X-ray Diffractometer (XRD) with Cu Kα irradiation ($\lambda = 1.54$ Å) range (diffraction angles (2θ)) from 5° to 80° with a step size of 2°/step and exposure time of 1 s/step.

3 Results and Discussion

3.1 Oxalate pyrite- alginate beads composite characterization

The as-prepared pyrite-alginate beads composite's physical imaging and diameter size were determined using SEM and imageJ software, respectively. **Figure 1 a-c** shows that the beads composite has a spherical shape with porous ridges on its surface. The uneven porous surface structure of beads composite provides a higher surface area for the sorption site of heavy metal cations [23]. The similar morphology was also seen from previous studies, e.g., bentonite-alginate beads [22], hydroxyapatite-alginate beads [24], $MgFe_2O_4$-biochar based-lanthanum alginate [25], MOF-incorporated Cu-based-alginate beads [26], urea formaldehyde modified-alginate beads [23]. The calculated average diameter was 4.157 ± 0.132 mm. The average diameter shows a larger diameter compared to Pandey‘s work using bentonite-alginate with a diameter size of 2.76 mm. This might happen due to lower concentrations of sodium alginate and calcium chloride during co-precipitation that the previous study used with concentrations of 2% and 3.5%, respectively [22]. Furthermore, the chemical compositions of the as-prepared composite are determined by EDX analysis. Table 1 confirms that the oxalate pyrite was successfully coated by the alginate layers with the presence of carbon, iron, sulphur, and sodium elements in the composite beads.

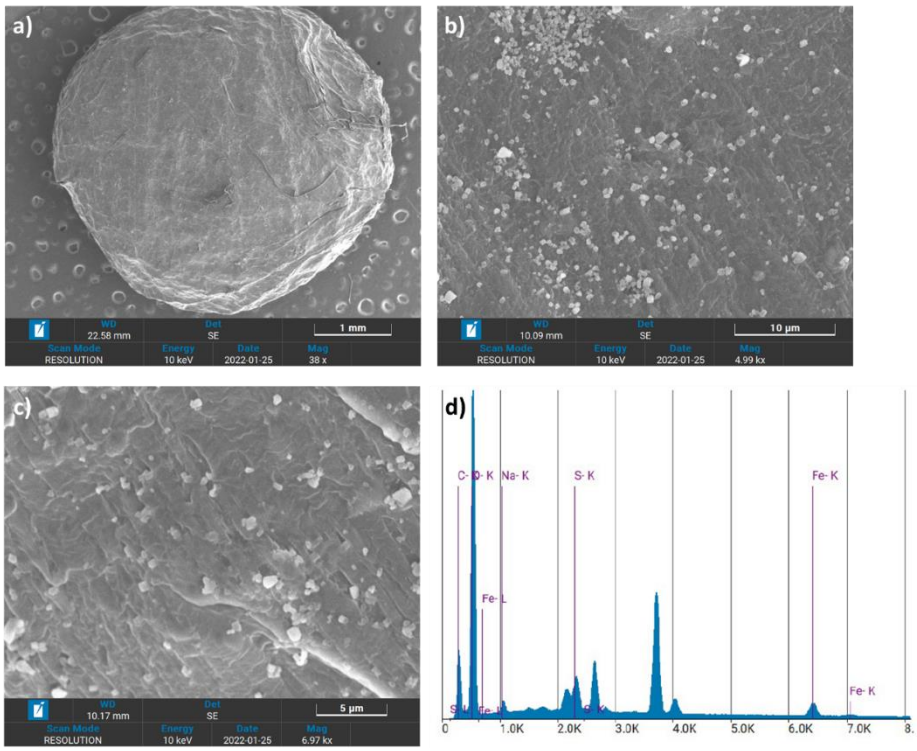

Fig. 1. SEM images of oxalate pyrite-alginate beads composite (a) 1 mm (b) 10 µm (c) 5 µm (d) EDX analysis

Table 1. EDX analysis of as-prepared oxalate pyrite-alginate beads composite

Element	Atomic %	Weight %
Carbon	48.50	40.02
Iron	0.33	1.26
Oxygen	48.46	53.27
Sodium	0.86	1.36
Sulphur	1.85	4.09

The functional group of as-prepared beads composite was investigated using FTIR analysis. The spectrum of oxalate pyrite-alginate beads composite is shown in **Figure 2**. The broad peak centered around 3275 cm^{-1} is ascribed to O-H bond stretching, indicating the presence of water molecules in the matrix [22], [27]. The prominent peaks at 1319, 1416, and 1599 cm^{-1}, which are denoted to stretching vibrations of symmetric and asymmetric bands of carboxylate anions [18], [28]. Moreover, the other prominent peaks (900-1250 cm^{-1}) centered at around 1000 cm^{-1} are attributed to the stretching band of S-S bonds that shows the pyrite facets [28]. Lastly, the presence of the peaks centered around 600 cm^{-1} is denoted by the stretching vibration of a Fe-S bond [27], [29].

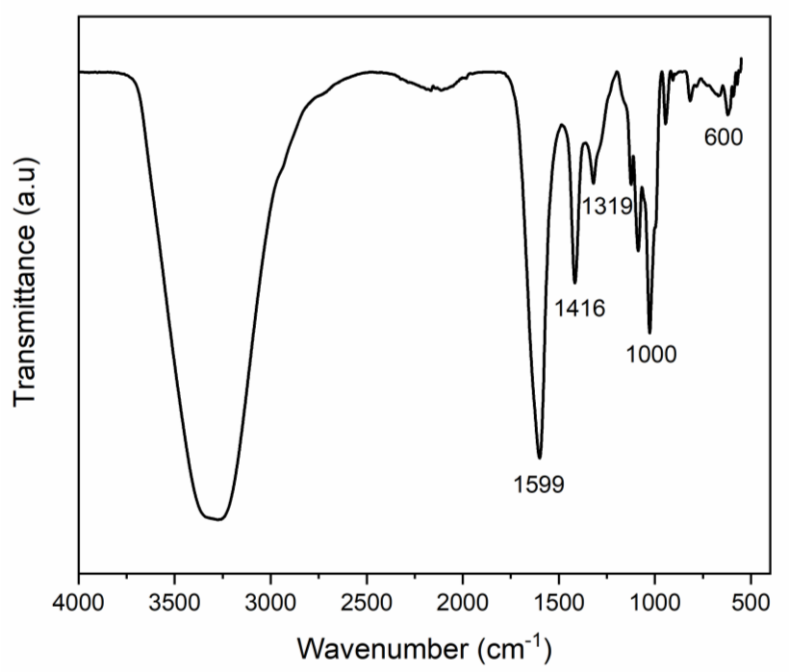

Fig. 2. FTIR spectra of oxalate pyrite-alginate beads composite

The crystallinity of the beads composite is determined using XRD analysis. The XRD spectrum of the oxalate pyrite-alginate beads composite is shown in **Figure 3**. The prominent peaks at 33.1°, 36.9°, 40.8°, 47.2°, 55.9°, 57.7°, 61.4°, and 63.8°correspond to plane indices of (200), (210), (211), (220), (311), (222), (023), and (321), respectively were confirmed to the cubic pyrite structure phase (JCPDS no. 42-1340) [27], [30], [31].

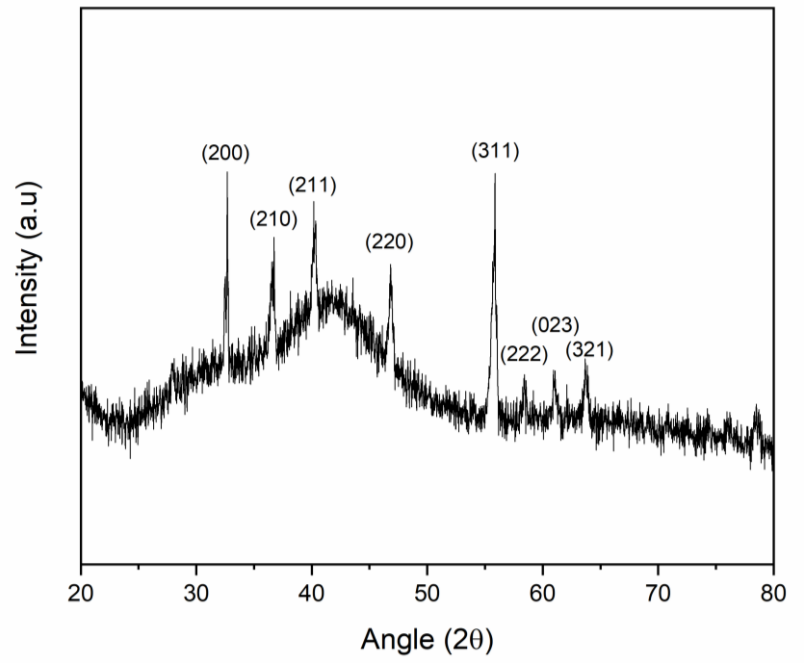

Fig. 3. XRD spectra of oxalate pyrite-alginate beads composite

3.2 Absorption performance

The absorption performance of oxalate pyrite-alginate beads composite is investigated using a copper in aqueous solution. **Figure 4** shows different absorbent dosages from 0.5 g to 3 g to determine the best performance by comparing the results. It was found that the dosage of 0.5, 1, 2, and 3 g exhibited 91.58%, 93.00%, 95.04%, and 96.28% removal from the aqueous environment after 8 h duration, respectively. It is found that the increase of 4.70% with the increase of dosage from 0.5 to 3 g. It is also denoted that at 3 g dosage, it is calculated that there is a 1.94% increase of copper removal from 2 to 8 h of duration.

Moreover, the best-performing beads composite dosage is evaluated to determine the capabilities to remove copper at a higher concentration. As seen from **Figure 5**, different copper solution concentrations, i.e. 5, 10, 15, and 20 ppm are used. It is discovered that the removal percentage are 96.66%, 96.25%, 96.17%, and 96.02% for 5, 10, 15, and 20 ppm copper concentrations, respectively. The decrease in removal performance is less than 1% from 5 ppm to 20 ppm. It shows that the oxalate pyrite-alginate beads composite have an excellent absorption property towards copper in an aqueous environment. It shows a higher possibility that the beads composite can be utilized at higher copper concentrations.

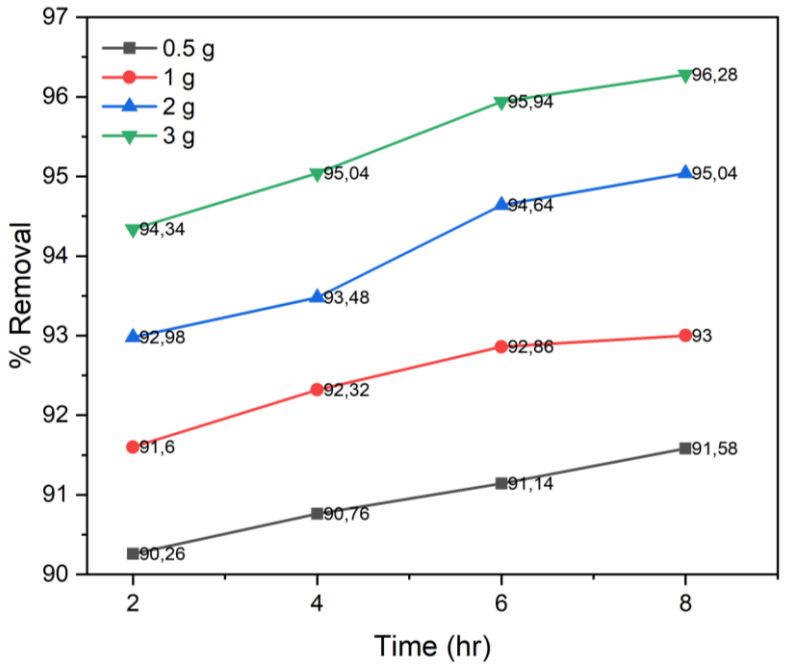

Fig. 4. Absorption performance of oxalate pyrite-alginate beads composite by different absorbent dosages

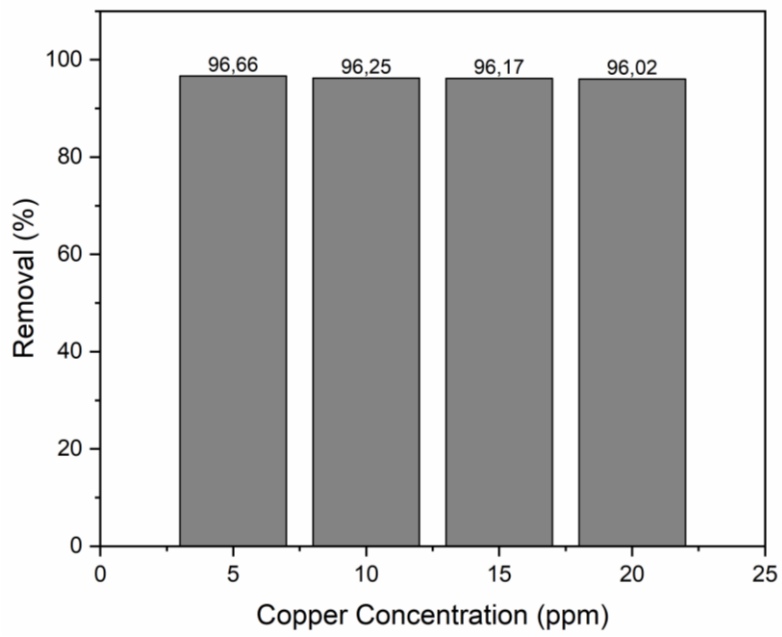

Fig. 5. Absorption performance of oxalate pyrite-alginate beads composite by different copper concentrations

The experimental data of the as-prepared composite is analyzed using isotherms plotted into linear isotherms of the Langmuir and Freundlich model that can be seen in Eq. 1 and Eq. 2, respectively [22], [32].

$$\frac{C_e}{q_e} = \frac{C_e}{q_m} + \frac{1}{K_L\, q_m} \tag{1}$$

$$\ln q_e = \ln K_F + \frac{1}{n} \ln C_e \tag{2}$$

Where C_e, q_e, q_m, K_L, and K_F are equilibrium concentration (mg/L), the amount of Cu^{2+} adsorbed (mg/g) , maximum uptake of Cu^{2+} per unit mass of adsorbent, Langmuir constant (L/mg), and Freundlich constant ((mg/g) $(L/mg)^{1/n}$) respectively.

Figure 6 shows the analysis of the adsorption isotherms by fitting into Freundlich and Langmuir's isotherm models. Based on the linear regression plotted for both Langmuir and Freundlich isotherm models, the Freundlich isotherm model calculated R^2 was 0.9965, and Langmuir only had R^2 of 0.1166. Thus, the adsorption of copper by using oxalate pyrite-alginate beads was best fitted into the Freundlich isotherm model. This model shows that the adsorption might favour a multilayer cooperative adsorption process [22]. The adsorption capacity obtained from the data is 4.00 mg/g.

Furthermore, the reusability of the beads composite is determined using 5 cyclic tests. **Figure 7** shows that the copper removal after the second to the fifth cycle is 90.34%, 90.34%, 82.06%, 75.00%, and 66.40%, respectively. It is found that the beads composite has relatively high stability with only a 23.94% decrease in performance. The decrease in performance occurred due to the swelling-shrinking of the beads composite after the fifth consecutive cyclic test [22].

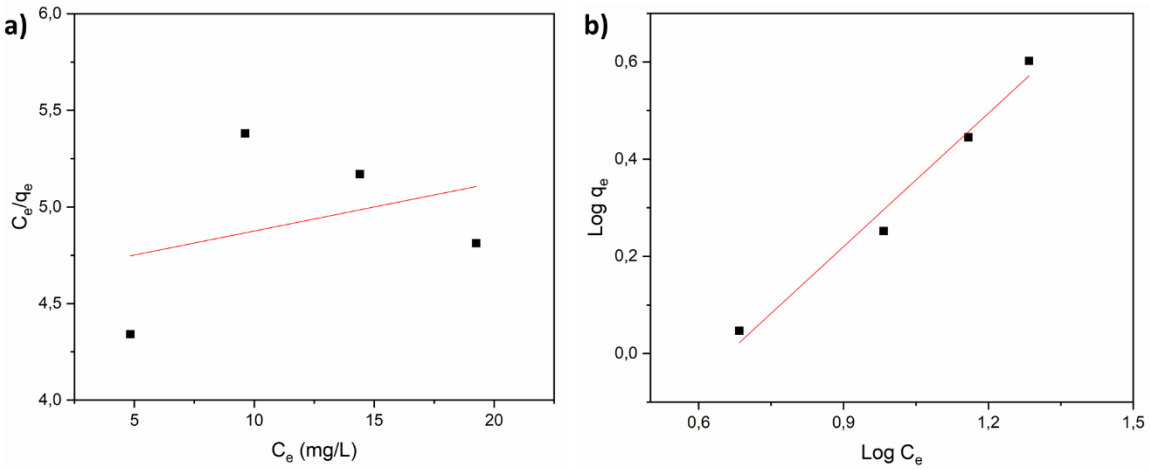

Fig. 6. Absorption isotherms of oxalate pyrite-alginate beads composite (a) Langmuir (b) Freundlich model

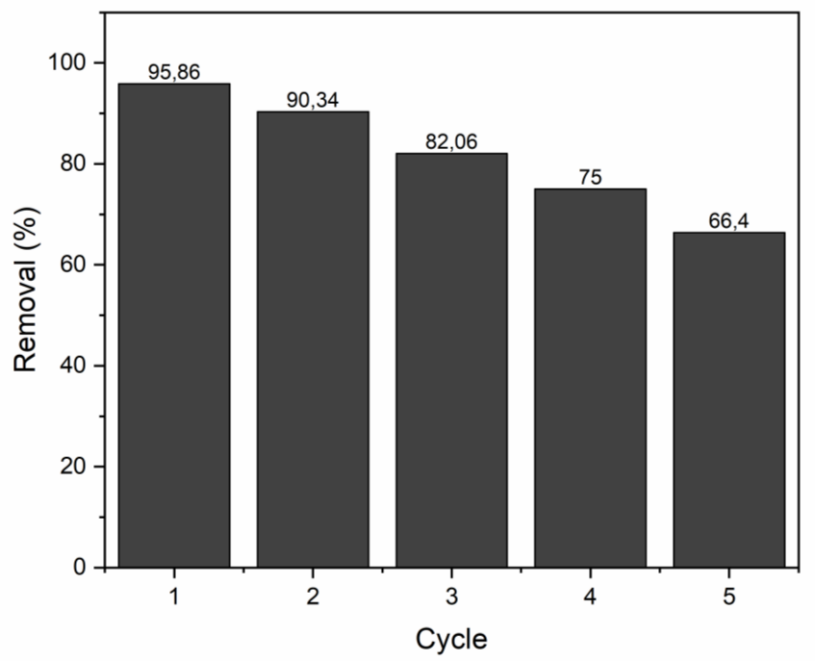

Fig. 7. Recyclability oxalate pyrite-alginate beads composite

4 Conclusion

In this present work, the development of oxalate pyrite encapsulated alginate beads was successfully prepared. The as-prepared oxalate pyrite-alginate beads composite exhibited a spherical structure and porous ridges surface with an average diameter of 4.157 ± 0.132 mm. The composite shows a high affinity toward copper absorption with 96.66% removal for 5 ppm concentration and high reusability with only a 23.94% decrease in removal after the fifth consecutive cycle. The Freundlich model isotherm is best fitted with q_m 4.00 mg/g.

REFERENCE

[1] R. Manne, M. M. R. M. Kumaradoss, R. S. R. Iska, A. Devarajan, and N. Mekala, "Water quality and risk assessment of copper content in drinking water stored in copper container," Appl Water Sci, vol. 12, no. 3, pp. 1–8, Mar. 2022, doi: 10.1007/S13201-021-01542-X.

[2] W. C. Poon, G. Herath, A. Sarker, T. Masuda, and R. Kada, "River and fish pollution in Malaysia: A green ergonomics perspective," Appl Ergon, vol. 57, pp. 80–93, Nov. 2016, doi: 10.1016/J.APERGO.2016.02.009.

[3] P. P. Leal et al., "Copper pollution exacerbates the effects of ocean acidification and warming on kelp microscopic early life stages," Scientific Reports 2018 8:1, vol. 8, no. 1, pp. 1–13, Oct. 2018, doi: 10.1038/s41598-018-32899-w.

[4] Ihsanullah et al., "Heavy metal removal from aqueous solution by advanced carbon nanotubes: Critical review of adsorption applications," Sep Purif Technol, vol. 157, pp. 141–161, Jan. 2016, doi: 10.1016/J.SEPPUR.2015.11.039.

[5] R. H. Harharah, G. M. T. Abdalla, A. Elkhaleefa, I. Shigidi, and H. N. Harharah, “A Study of Copper (II) Ions Removal by Reverse Osmosis under Various Operating Conditions,” Separations 2022, Vol. 9, Page 155, vol. 9, no. 6, p. 155, Jun. 2022, doi: 10.3390/SEPARATIONS9060155.
[6] A. Janin, L. Coudert, G. Mercier, and J. F. Blais, “Copper extraction and recovery from alkaline copper quaternary and copper azole treated wood using sulfuric acid leaching and ion exchange or electrodeposition,” J Clean Prod, vol. 279, p. 123687, Jan. 2021, doi: 10.1016/J.JCLEPRO.2020.123687.
[7] H. Hu, X. Li, P. Huang, Q. Zhang, and W. Yuan, “Efficient removal of copper from wastewater by using mechanically activated calcium carbonate,” J Environ Manage, vol. 203, pp. 1–7, Dec. 2017, doi: 10.1016/J.JENVMAN.2017.07.066.
[8] J. Ju et al., “Separation of Cu, Co, Ni and Mn from acid leaching solution of ocean cobalt-rich crust using precipitation with Na2S and solvent extraction with N235,” Korean Journal of Chemical Engineering 2022 39:3, vol. 39, no. 3, pp. 706–716, Jan. 2022, doi: 10.1007/S11814-021-0919-9.
[9] J. Khan, S. Lin, J. C. Nizeyimana, Y. Wu, Q. Wang, and X. Liu, “Removal of copper ions from wastewater via adsorption on modified hematite (α-Fe2O3) iron oxide coated sand,” J Clean Prod, vol. 319, p. 128687, Oct. 2021, doi: 10.1016/J.JCLEPRO.2021.128687.
[10] B. Song et al., “Pyrite-mediated advanced oxidation processes: Applications, mechanisms, and enhancing strategies,” Water Res, vol. 211, p. 118048, Mar. 2022, doi: 10.1016/J.WATRES.2022.118048.
[11] Y. Yang, J. Liu, F. Liu, Z. Wang, and S. Miao, “Molecular-level insights into mercury removal mechanism by pyrite,” J Hazard Mater, vol. 344, pp. 104–112, Feb. 2018, doi: 10.1016/J.JHAZMAT.2017.10.011.
[12] C. Kantar, C. Ari, S. Keskin, Z. G. Dogaroglu, A. Karadeniz, and A. Alten, “Cr(VI) removal from aqueous systems using pyrite as the reducing agent: Batch, spectroscopic and column experiments,” J Contam Hydrol, vol. 174, pp. 28–38, Mar. 2015, doi: 10.1016/J.JCONHYD.2015.01.001.
[13] N. A. Abdul, S. Abdul-Talib, and A. Amir, “Nano-pyrite as a Reductant to Remove Chromium in Groundwater,” KSCE Journal of Civil Engineering 2019 23:3, vol. 23, no. 3, pp. 992–999, Jan. 2019, doi: 10.1007/S12205-019-1034-X.
[14] Y. Chen et al., “Efficient removal of Cr(VI) from aqueous solution by natural pyrite/rhodochrosite derived materials: Performance, kinetic and mechanism,” Advanced Powder Technology, vol. 32, no. 10, pp. 3814–3825, Oct. 2021, doi: 10.1016/J.APT.2021.08.032.
[15] A. Özverdi and M. Erdem, “Cu2+, Cd2+ and Pb2+ adsorption from aqueous solutions by pyrite and synthetic iron sulphide,” J Hazard Mater, vol. 137, no. 1, pp. 626–632, Sep. 2006, doi: 10.1016/J.JHAZMAT.2006.02.051.
[16] B. Yang, X. Tong, Z. Deng, and X. Lv, “The adsorption of Cu species onto pyrite surface and its effect on pyrite flotation,” J Chem, vol. 2016, 2016, doi: 10.1155/2016/4627929.
[17] X. Gao, C. Guo, J. Hao, Z. Zhao, H. Long, and M. Li, “Adsorption of heavy metal ions by sodium alginate based adsorbent-a review and new perspectives,” Int J Biol Macromol, vol. 164, pp. 4423–4434, Dec. 2020, doi: 10.1016/J.IJBIOMAC.2020.09.046.
[18] I. T. K. Ge, M. W. Nugraha, N. Ahmad Kamal, and N. S. Sambudi, “Composite of Kaolin/Sodium Alginate (SA) Beads for Methylene Blue Adsorption,” ASEAN Journal of Chemical Engineering, vol. 19, no. 2, pp. 100–109, Jan. 2020, doi: 10.22146/AJCHE.51457.
[19] Y. Zhao, L. Zhan, Z. Xue, K. K. Yusef, H. Hu, and M. Wu, “Adsorption of Cu (II) and Cd (II) from Wastewater by Sodium Alginate Modified Materials,” J Chem, vol. 2020, 2020, doi: 10.1155/2020/5496712.
[20] A. Sharma, D. Baral, H. B. Bohidar, and P. R. Solanki, “Oxalic acid capped iron oxide nanorods as a sensing platform,” Chem Biol Interact, vol. 238, pp. 129–137, Aug. 2015, doi: 10.1016/J.CBI.2015.05.020.

[21] A. Sun, H. Zhao, M. Wang, J. Ma, H. Jin, and K. Zhang, "One-Pot Synthesis of Pyrite Nanoplates Supported on Chitosan Hydrochar as Fenton Catalysts for Organics Removal from Water," Catalysts, vol. 12, no. 8, p. 858, Aug. 2022, doi: 10.3390/CATAL12080858/S1.
[22] Ravi and L. M. Pandey, "Enhanced adsorption capacity of designed bentonite and alginate beads for the effective removal of methylene blue," Appl Clay Sci, vol. 169, pp. 102–111, Mar. 2019, doi: 10.1016/J.CLAY.2018.12.019.
[23] P. Qu et al., "Urea formaldehyde modified alginate beads with improved stability and enhanced removal of Pb2+, Cd2+, and Cu2+," J Hazard Mater, vol. 396, p. 122664, Sep. 2020, doi: 10.1016/J.JHAZMAT.2020.122664.
[24] J. Iqbal et al., "Synergistic effects of activated carbon and nano-zerovalent copper on the performance of hydroxyapatite-alginate beads for the removal of As3+ from aqueous solution," J Clean Prod, vol. 235, pp. 875–886, Oct. 2019, doi: 10.1016/J.JCLEPRO.2019.06.316.
[25] L. Wang, J. Wang, W. Yan, C. He, and Y. Shi, "MgFe2O4-biochar based lanthanum alginate beads for advanced phosphate removal," Chemical Engineering Journal, vol. 387, p. 123305, May 2020, doi: 10.1016/J.CEJ.2019.123305.
[26] S. J. Lee, T. Hann, and S. H. Park, "Seawater Desalination Using MOF-Incorporated Cu-Based Alginate Beads without Energy Consumption," ACS Appl Mater Interfaces, vol. 12, no. 14, pp. 16319–16326, Apr. 2020, doi: 10.1021/ACSAMI.9B22843/.
[27] C. K. Das et al., "Nano-pyrite seed dressing: a sustainable design for NPK equivalent rice production," Nanotechnology for Environmental Engineering, vol. 3, no. 1, pp. 1–14, Dec. 2018, doi: 10.1007/S41204-018-0043-1/.
[28] Z. Wang, J. Cao, L. Wang, J. Xiao, and J. Wang, "Selective depression of arsenopyrite with in situ generated nanoparticles in pyrite flotation," Miner Eng, vol. 173, p. 107223, Nov. 2021, doi: 10.1016/J.MINENG.2021.107223.
[29] F. Rahimi, J. P. van der Hoek, S. Royer, A. Javid, A. Mashayekh-Salehi, and M. Jafari Sani, "Pyrite nanoparticles derived from mine waste as efficient catalyst for the activation of persulfates for degradation of tetracycline," Journal of Water Process Engineering, vol. 40, p. 101808, Apr. 2021, doi: 10.1016/J.JWPE.2020.101808.
[30] S. C. Mangham, M. Alam Khan, M. Benamara, and M. O. Manasreh, "Synthesis of iron pyrite nanocrystals utilizing trioctylphosphine oxide (TOPO) for photovoltaic devices," Mater Lett, vol. 97, pp. 144–147, Apr. 2013, doi: 10.1016/J.MATLET.2013.01.101.
[31] S. Khalid et al., "Transition metal doped pyrite (FeS 2) thin films: structural properties and evaluation of optical band gap energies," J Mater Chem C Mater, vol. 3, no. 46, pp. 12068–12076, Nov. 2015, doi: 10.1039/C5TC03275J.
[32] K. Chung Hui, W. Lun Ang, and N. Soraya Sambudi, "Nitrogen and bismuth-doped rice husk-derived carbon quantum dots for dye degradation and heavy metal removal," J Photochem Photobiol A Chem, vol. 418, p. 113411, Sep. 2021, doi: 10.1016/J.JPHOTOCHEM.2021.113411.